Detecting protein aggregation and interactions in live cells: a guide to Number and Brightness

Article *in* Methods · December 2017

DOI: 10.1016/j.ymeth.2017.12.001

4 authors:

Sergi Padilla-Parra
University of Oxford
88 PUBLICATIONS **572** CITATIONS
SEE PROFILE

Rory Nolan
University of Oxford
12 PUBLICATIONS **17** CITATIONS
SEE PROFILE

Maro Iliopoulou
University of Oxford
6 PUBLICATIONS **4** CITATIONS
SEE PROFILE

Luis A J Alvarez
University of Oxford
29 PUBLICATIONS **371** CITATIONS
SEE PROFILE

Methods xxx (2017) xxx–xxx

Contents lists available at ScienceDirect

Methods

journal homepage: www.elsevier.com/locate/ymeth

Detecting protein aggregation and interaction in live cells: A guide to number and brightness

Rory Nolan [a], Maro Iliopoulou [a], Luis Alvarez [a], Sergi Padilla-Parra [a,b,*]

[a] Wellcome Centre Human Genetics, University of Oxford, Oxford OX3 7BN, UK
[b] Division of Structural Biology, University of Oxford, The Henry Wellcome Building for Genomic Medicine, Headington, Oxford OX3 7BN, UK

ARTICLE INFO

Article history:
Received 15 September 2017
Received in revised form 1 December 2017
Accepted 3 December 2017
Available online xxxx

ABSTRACT

The possibility to detect and quantify protein-protein interactions with good spatial and temporal resolutions in live cells is crucial in biology. Number and brightness is a powerful approach to detect both protein aggregation/desegregation dynamics and stoichiometry in live cells. Importantly, this technique can be applied in commercial set ups: both camera based and laser scanning microscopes. It provides pixel-by-pixel information on protein oligomeric states. If performed with two colours, the technique can retrieve the stoichiometry of the reaction under study. In this review, we discuss the strengths and weaknesses of the technique, stressing which are the correct acquisition parameters for a given microscope, the main challenges in analysis, and the limitations of the technique.

Contents

1. Introduction: fluorescence microscopy and detecting protein interactions

To better understand different biological functions within the cell (e.g. receptor dynamics, signal transduction or chromatin dynamics) it is of principal importance to describe how proteins interact with each other. Traditionally, *in vitro* biophysical assays

* Corresponding author at: Wellcome Centre Human Genetics, University of Oxford, Oxford OX3 7BN, UK.
E-mail address: spadilla@well.ox.ac.uk (S. Padilla-Parra).

https://doi.org/10.1016/j.ymeth.2017.12.001
1046-2023/

have been used to characterize protein interactions, but recently, a myriad of different fluorescence microscopy techniques have been applied for this purpose *in vitro* and in live cells. Within this family, we review number and brightness [1] which belongs to the field of fluorescence fluctuation spectroscopy (FFS). Number and brightness (N&B) applies moment analysis [2,3] to measure the average number and brightness of labelled entities in each pixel of a stack of fluorescence microscopy images. These quantities give information on the concentration of these entities and their oligomeric state. These images may be acquired with a simple laser scanning microscope (LSM, with either digital or analog detectors) or a camera-based fluorescence microscope, for example, a total internal reflection (TIRF) microscope [4,5]. One advantage of fluorescence fluctuation approaches is that they require relatively low concentrations of labelled protein (in the range of nM, [6]), therefore issues related to protein over-expression [6] can be avoided. An caveat of N&B is that it functions correctly for diffusive entities only and therefore cases with a subpopulation of immobile particles cannot be well-quantified. As with many fluorescence microscopy-based approaches, the rate of photobleaching will affect quantification and, if not properly addressed, will confound the final results [7].

2. Number and brightness in the current biological context: the CRISPR era

The quantification of protein interactions at endogenous levels of proteins is essential to unveil the biological function at the molecular level in a living cell. Conventionally, immunostaining and over-expression of fluorescently-tagged proteins have been used to quantify protein interactions. Both of these methods have their caveats: immunostaining with primary or secondary antibodies can lack specificity [8] and hence must be performed and interpreted with great care, and over-expression can cause changes in cell function and induce artificial protein interactions [9] by forcing protein contacts through crowding. Several strategies have been devised to overcome these issues in single cells, e.g. recombinant antibody-like proteins [10] and conditional tag knocking strategies [11]. Genome editing, which allows manipulation of the genome *in vivo* to insert a tag sequence of a fluorescent protein into the gene of interest, offers great promise to solve these problems. CRISPR-Cas9 [12–14] permits fluorescent labelling of endogenous proteins and is most likely the best system to quantify protein interactions at endogenous expression levels in live cells. CRISPR-Cas9 endogenously labelled samples have been imaged using laser scanning confocal microscopy [15], and super-resolution techniques (PALM and dSTORM) have also been applied [16–18]. We anticipate that FFS approaches – N&B in particular – will become very attractive for CRISPR-Cas9 engineered cell lines expressing endogenous levels of labelled proteins, because they work well with dim (lowly-expressing) samples.

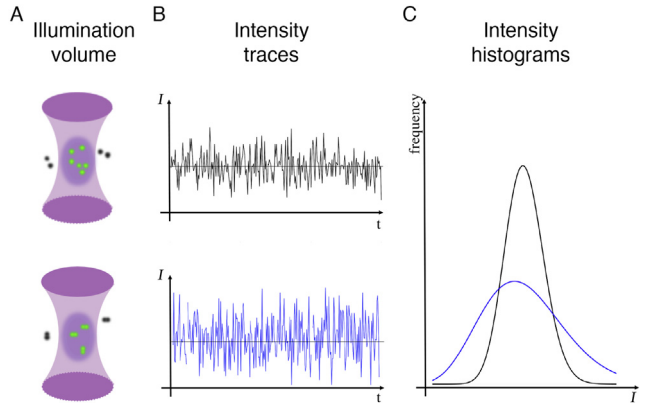

Fig. 1. Consider a system in which monomeric proteins undergo dimerization. A. Row 1: prior to dimerization, an average of 6 monomers are excited in the observation volume. Row 2: after dimerization, an average of 3 dimers are excited in the observation volume. We have the same concentration of fluorophores and therefore the same intensity average, however after dimerization, we have a higher variance in intensity. This is because now the fluorophores are entering and leaving the observation volume two at a time. B&C. This constant mean and increase in variance is seen in the intensity traces and the intensity histograms (monomers in black, dimers in blue). The widening of the histogram in the dimeric (blue) case shows the increase in variance. (For interpretation of the references to colour in this figure legend, the reader is referred to the web version of this article.)

3. Number and brightness, theory and analysis

Before discussing the strengths and weaknesses of N&B in live cells, we introduce the mathematical concepts first described by Digman et al. [1] (Fig. 1). Define an *entity* as a set of molecules which are chemically bound and the brightness ϵ of an entity as the mean number of photon detector counts it gives per unit time when in the illumination volume. For an image series where the i^{th} slice in the stack is the image acquired at time $t = i$, for a given pixel position (x, y), we define $\langle I \rangle$ as the mean intensity of that pixel over the image series and σ^2 as the variance in that intensity. Define n as the mean number of entities in the illumination volume corresponding to that pixel. If we are in photon-counting mode with zero background and all entities are mobile, we have

$$N = \frac{\langle I \rangle^2}{\sigma^2} = \frac{\epsilon n}{1 + \epsilon}$$

$$B = \frac{\sigma^2}{\langle I \rangle} = 1 + \epsilon$$

where N and B are referred to as the "apparent number" and "apparent brightness" respectively. This gives

$$n = \frac{\langle I \rangle^2}{\sigma^2 - \langle I \rangle}$$

$$\epsilon = \frac{\sigma^2}{\langle I \rangle} - 1$$

These relations are derived using a moment analysis technique which was originally applied to molecules in solution by Qian and Elson [19]. Dalal et al. [20] showed that with a scanning confocal microscope in analog mode, we must use three correction terms: 1. The proportionality constant S, which is the conversion factor between photons detected and the number of counts returned by the analog electronics. That is, if the analog electronics give c_a counts, then this corresponds (on average) to $S \times c_a$ photons detected. 2. The offset (bias) due to the analog electronics in the level of the background. 3. The readout noise σ_0^2 is the variance in this background signal. Then, if all entities are mobile, we have

$$N = \frac{(\langle I \rangle - \text{offset})^2}{\sigma^2 - \sigma_0^2} = \frac{\epsilon n}{1 + \epsilon}$$

$$B = \frac{\sigma^2 - \sigma_0^2}{\langle I \rangle - \text{offset}} = S(1 + \epsilon)$$

which give

$$n = \frac{(\langle I \rangle - \text{offset})^2}{\sigma^2 - \sigma_0^2 - S(\langle I \rangle - \text{offset})}$$

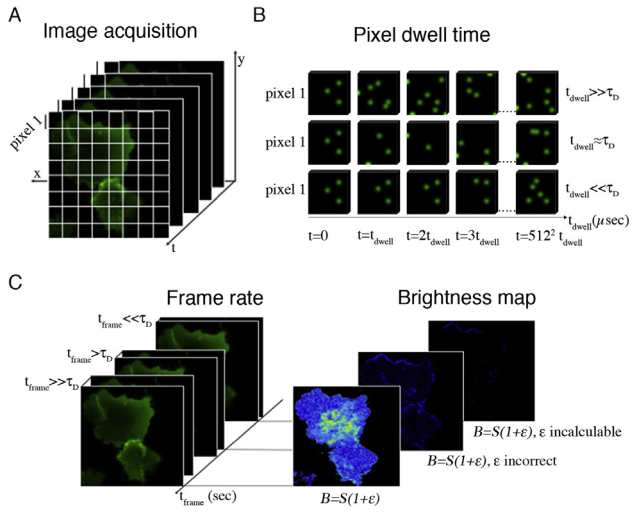

Fig. 2. A. Stack of images showing pixel 1 in each image. B. We need $t_{dwell} \ll \tau_D$ so that the particle configuration is approximately constant during the course of a dwell. Indeed in row 3, we see that with $t_{dwell} \ll \tau_D$, even after $3t_{dwell}$ has passed, the configuration has not changed significantly. In the other rows ($t_{dwell} \approx \tau_D$ and $t_{dwell} \gg \tau_D$), we see that the particle configuration is changing significantly during the course of a dwell, such that at $t = 0$ and $t = t_{dwell}$ we have different configurations. B&C. After a whole frame (e.g. 512×512 pixels), we need the particle configuration to have changed to another random configuration. This is the requirement $t_{frame} \gg \tau_D$ where in our 512×512 pixel example, $t_{frame} > 512^2 t_{dwell}$. If this requirement is not satisfied, we either incorrectly underestimate ϵ (in the case $t_{frame} \approx \tau_D$) or we go so fast that everything appears immobile (case $t_{frame} \ll \tau_D$) and we cannot calculate a value for ϵ.

$$\epsilon = \frac{\sigma^2 - \sigma_0^2 - S(\langle I \rangle - \text{offset})}{\langle I \rangle - \text{offset}}$$

Instructions on how to measure S, σ_0^2 and offset are also given by Dalal et al. [20]. Note that photon counting mode with background is equivalent to analog mode with $S = 1$ and with σ_0^2 and offset measured in the same way as for an analog system [20].

When operating in analog mode, the dynamic range is diminished (relative to photon counting mode), limiting quantitative determination of relative aggregate sizes to those that are within a factor of 2–10 in brightness. The results in analog mode are also highly sensitive to detector instability [20].

4. Immobility and the speed of acquisition in number and brightness

For immobile entities, we get $B = 1$ in photon counting mode with no background or $B = S$ in analog mode, so we cannot determine ϵ from B. If a pixel has a mixture of mobile and immobile entities, then the calculated B will be somewhere between its mobile and immobile value for the entities in that pixel, again rendering ϵ incalculable. However, in this case, B will still increase upon an increase in oligomeric state of the mobile entities, and thus the technique can still be used to detect changes in oligomeric state (but not to quantify the oligomeric state). When a particle is said to be *immobile*, what is meant is that particle moves slowly enough such that it tends to remain in a given observation volume (a given pixel) over the course of the acquisition (Fig. 2). *Mobile* particles, on the other hand, tend to leave a given observation volume from one observation to the next (they could even go out and come back in). When acquiring for N&B analysis, we want *mobile* particles. Hence, it is theoretically possible to acquire at a frame rate which is too fast: if your frame time is extremely short, then the entities will not move appreciably in that time, so they will all appear as immobile, and thus ϵ will be incalculable. Let τ_D be the characteristic residence time: the average time that a particle which enters the focal volume remains in that volume. Then, the frame rate requirement is $t_{frame} \gg \tau_D$, where t_{frame} is the time taken to acquire a frame (more specifically, the time between the acquisition of the first pixel of a given frame and the acquisition of the first pixel of the next frame).

Even though our *frame rate* does not need to be fast, we do need the pixel *dwell time* t_{dwell} to be short enough such that we are sampling one and only one configuration of particles in the focal volume, i.e. that the probability of a particle entering or exiting the focal volume over the course of a dwell is very small. This requirement can be expressed mathematically as $t_{dwell} \ll \tau_D$. The time taken to capture a frame is equal to the sum of the times taken to capture all of the pixels plus some preparation time to prepare capture of the next frame. Hence, for a frame size of p pixels (where p is relatively large e.g. $512 \times 512 \approx 2.6 \times 10^5$), we have $t_{frame} \geqslant p t_{dwell}$ and hence $t_{frame} \gg t_{dwell}$ and thus the overall requirement $t_{frame} \gg \tau_D \gg t_{dwell}$ can readily be satisfied if τ_D is approximately known. This is described in Fig. 2.

As an example, suppose we have a protein diffusing in the plasma membrane with known diffusion constant $D = 1\ \mu m^2/s$ and a focal volume with waist $w_{xy} = 0.25\ \mu m$. Suppose we wish to perform N&B analysis on this protein with 128×128 pixel images. Fluorescence correlation spectroscopy (FCS) theory gives us the relation $\tau_D = \frac{w_{xy}^2}{4D}$, which gives in our example $\tau_D \approx 0.0156$ s. Now, if we choose a dwell time $t_{dwell} = 10\ \mu s$, we get $t_{frame} \geq 128^2 t_{dwell} \approx 0.16$ s, and hence the requirement $t_{frame} \gg \tau_D \gg t_{dwell}$ is satisfied.

If your minimum achievable dwell time is too long, then there is no remedy. If your frame time t_{frame} is too short, it can be artificially increased by pausing between frames (or discarding frames).

5. Separating the mobile and immobile contributions

Digman et al. [1] showed that in images where some pixels contain only mobile entities and the other pixels have only immobile entities, these can be delimited with the knowledge that, upon an increase in laser power, only the pixels with mobile entities will see an increase in brightness B. This should be done with care, however, because if there are pixels with a mixture of mobile and immobile entities, then these will also see an increase in brightness B (albeit with a smaller increase than those pixels with mobile entities only). Indeed, we have never seen – in live cells – an example of where this kind of correction is applicable (because if there are mobile and immobile entities, they tend to be somewhat co-located). Hence, we do not recommend this approach in live cells.

Dalal et al. [20] showed that if one can determine the ratio R of the immobile to mobile intensity contribution at each pixel, then one can correct for the immobile contribution and the brightness ϵ can be satisfactorily recovered. However, the determination of this ratio R at each pixel is unfeasible. It is tempting to use FRAP (fluorescence recovery after photobleaching) to bleach away the immobile part and to measure the mobile part as what remains after recovery, but this relies on the assumption that mobile particles do not bleach. This assumption is common in N&B analysis, justified as passable by the idea that "bleached, mobile molecules will be replaced with unbleached molecules" [1]. This ignores the fact that bleaching mobile molecules reduces the overall supply of mobile molecules, which implies that a full replacement cannot be assumed. Hence, neither do we recommend this attempt to separate the mobile and immobile contributions.

6. Frame rate in Imaging FCS and FFS

In Imaging FCS [21], there is an intrinsic need to acquire at high frame rates because there, we are attempting to measure

correlation over time, so we need to go fast enough such that the system has undergone only a slight change of state from one time point to the next, so that these consecutive time points are somewhat *correlated*. N&B is a fluorescence *fluctuation* spectroscopy (FFS) technique. FFS is unconcerned with correlation and thereby FFS techniques are free from this requirement of rapid frame rates. Indeed, in N&B, we treat each time point as a random configuration of the system, unrelated to the previous and next time points. This can be better understood by considering that, for the purpose of N&B, we may arbitrarily permute the time points without changing the result: this will not change the quantities $\langle I \rangle$ or σ^2 which are the only quantities (apart from S, σ_0^2 and offset, which are all properties of the acquisition system) needed to calculate n and ϵ. Conversely, permuting time points would be disastrous in FCS.

7. Photobleaching in number and brightness

Photobleaching/photodepletion (henceforth referred to as "bleaching") of the fluorophores in the sample leads to a decrease in mean intensity over time. The N&B calculations above implicitly rely on the sample having a stationary mean fluorescence. When this assumption is broken, the calculated pixel intensity means and variances are altered, rendering the N&B calculations useless. Bleaching is unavoidable, so a correction for this effect is desirable. This correction either involves modelling the bleaching into the N&B calculations, or detrending the data (computationally removing the trend in the data caused by bleaching) prior to preforming the N&B calculations. Theoretically, bleaching should occur in a manner such that the fluorescence decreases according to an exponential decay. Hur et al. [22] show that this can be the case in practice and they show how to correct for bleaching of this kind by including an exponential decay bleaching model into the N&B calculations. If the bleaching curve is indeed an exponential decay, then this is the ideal method. There are, however, many cases in which the bleaching does not follow an exponential decay regime (see experimental data in Nolan et al. [7] for some examples). A more flexible approach is to use a polynomial of low degree to fit (and remove) the trend in the data. This method suffers from the fact that the tuning parameter – the degree of the polynomial – is discrete and the fit can differ significantly from one degree to the next, with nothing in between. Nonetheless, this technique can work well in practice and has been in widespread use for detrending time series data for decades [23].

Non-fitting approaches to bleaching correction have the advantage that they do not rely on the experimental fluorescence decay curve being well-fit by any particular function type. Both of the popular non-fitting approaches may be described as *moving average* approaches. They calculate, for each point in the time series (each pixel is its own time series of intensity values), a *local average* of that point and its neighbouring time-points. Then, the *fluctuation* at that point is defined as its deviation from this local average, and the point's value is then reset to the global average for that time series plus this fluctuation value. There are two methods of calculating this local average. The first is the box-car method (sometimes referred as the *sliding window* or just *moving average*). This method sets the local average equal to the mean of the value of the given point and its $2l$ nearest neighbours (l on either side). The second method is *exponential filtering*. Here, the local average is a weighted average weighted by an exponential function with parameter τ whereby the weights get smaller with increasing distance from the point of interest. This method was advocated by Digman et al. [1] and is described in detail in the Supplementary Material of Nolan et al. [7]. The polynomial detrend and both moving average methods above require the user to choose a parameter (the degree p of the polynomial, the size parameter l of the box and the exponential parameter τ respectively). We have shown [7] how to correctly choose the value of these parameters by exploiting the fact that immobile entities give $B = 1$ (or $B = S$). We also showed that the correct choice of the parameter is crucial because in some cases, different choices of this parameter can lead to drastically different results.

Users of bleaching correction should be aware that bleaching correction is difficult and only works well when a small degree (definitely <20%) of bleaching has occurred. We [7] showed through simulations the surprising result that in many cases, having no bleaching correction at all can work better. Hur and Mueller [22] discuss the effects of different degrees of bleaching in detail, showing that the effect of bleaching depends on intensity and on fluorophore concentration.

Aside from introducing a non-stationary mean, bleaching causes another problem: if some fluorophores are bleached, this can cause, for example, a trimer to appear like a dimer because only two of its three fluorophores are functioning. This problem requires another kind of correction. Let ϵ_0 be the brightness ϵ that would have been measured in the absence of bleaching (i.e. ϵ_0 is the quantity we want) and let ϵ_m be the actual brightness ϵ that we measured (in the presence of bleaching). Let F_0 be the initial intensity level (measured by the mean intensity of the first frame) and let F_T be the final intensity level (mean intensity of the last frame). Now we may define the photodepletion fraction $f_D = \frac{F_0 - F_T}{F_0}$ and we have

$$\epsilon_0 = \frac{\epsilon_m}{1 - \frac{f_D}{2}} - \frac{\frac{f_D}{2}}{1 - \frac{f_D}{2}}$$

This was derived by Hur and Mueller [22]. In the same paper, they discuss the idea of segmented brightness, which is to break up the image series into small chunks, perform brightness analysis on each chunk and then to average the results. This is done to negate the effects of bleaching. This is an interesting idea but will not be further discussed in this review.

8. Other corrections to number and brightness

Cell movement can confound N&B calculations. In particular, pixels in which the cell moved into or out of over the course of the acquisition need to be excluded.

The N&B technique implicitly assumes that the observation volume is in complete overlap with the sample. Macdonald et al. [24] demonstrate how to use the technique in samples that are too thin to satisfy this requirement by using z-scan fluorescence spectroscopy. The small volume of prokaryotic cells poses a similar problem. Hur and Mueller [25] developed mean segmented Q-value (MSQ) analysis for the purpose of doing N&B in prokaryotic cells, demonstrating the technique in *E. coli*.

If acquisition from two or more channels is being attempted, pulsed interleaved excitation (PIE) can be used to avoid bleed-through [26]. Digman et al. (2007) showed that in the (common) case of a non-uniform illumination profile characterized by point spread function PSF($\boldsymbol{r}$), the calculated number n must be adjusted according to the transformation $n \to n/\gamma$, where

$$\gamma = \frac{\int \mathrm{PSF}^2(\boldsymbol{r}) d^3 r}{\int \mathrm{PSF}(\boldsymbol{r}) d^3 r}$$

For a Gaussian illumination profile, $\gamma \approx 0.3536$, whereas for a Gaussian-Lorentzian illumination profile, $\gamma \approx 0.076$.

9. Fluorophores, laser power and number of frames

Brighter fluorophores are better for N&B. This is because for brighter fluorophores have a bigger ϵ, and hence the difference between ϵ and 2ϵ (i.e. the difference between monomers and dimers) is larger and therefore easier to detect, and so on for higher order oligomers. The brightness ϵ of a fluorophore can be increased by increasing the laser power, however this also increases the amount of bleaching, so there is a balance to strike. This balance can be hard to find and this can be a lengthy part of the setup of N&B experiments.

Another important aspect is the number of frames needed for an accurate pixel-by-pixel brightness computation. The error in the calculated number and brightness decreases with the square root of the number of acquired frames. Hence, the adequate number of frames depends on what is being investigated, and more frames always give greater accuracy (so long as other problems like over-bleaching don't occur over the longer acquisition). In the literature, as few as 20 frames have been used, whilst we have on occasion seen fit to use 1000 frames. The required number of frames will also depend on the photon budget (i.e. number of detected photons per pixel). With as few as 1–10 photons per pixel we recommend ≈500 frames to get reliable brightness values.

10. Summary of experimental parameters for N&B

- The laser power needs to be adjusted to minimize bleaching (try to bleach less than 20% of the total signal during the whole acquisition).
- The speed of the acquisition needs to satisfy $t_{\text{frame}} \gg \tau_D \gg t_{\text{dwell}}$.
- The number of total frames needs to be sufficient – depending on the photon budget – to allow for accurate N&B calculations (the lower the number of photons per frame, the higher the number of frames needed with about 500 frames needed for 1–10 photon counts per pixel per frame).

11. Extensions of number and brightness

The two colour version of N&B appeared right after the original publication in 2009 and was termed cross-correlated number and brightness (ccN&B) [27]. It extends N&B to study hetero-interactions (interaction of different proteins labelled with different fluorophores). This can be combined with conventional N&B done on each of the channels of the separate fluorophores to study the stoichiometry of the interactions of two proteins. When using two colours, attention must be paid to bleed-through between channels. For example, when using green and red fluorescent proteins, it is possible that photons from the green channel are counted twice; that is in the corresponding green channel but also in the red channel due to the long tails of the emission spectra for most of the green fluorescent proteins. This will artificially increase the cross-correlation and therefore could induce false positives for protein interactions. There are many ways to alleviate this problem [28]. For commercial laser scanning microscopy, we recommend line inter-leaved excitation which consists of sequentially scanning the green and red lines to avoid simultaneous excitation of both proteins. In camera-based approaches, we recommend pulsed inter-leaved excitation (PIE) [26,29].

Pair-correlation of molecular brightness (pCOMB) [30] combines N&B with pair correlation function (pCF) analysis [31] to study the movements of different oligomeric species within the same sample. Hinde et al. use this technique to demonstrate the different motilities of signal transducer and activator of transcription 3 (STAT3) dimers and tetramers.

12. Alternatives to number and brightness

Förster resonance energy transfer (FRET), the photon-counting histogram (PCH), FCS and spatial intensity distribution analysis (SpIDA) have all been used to detect oligomerization of fluorescently-tagged proteins. SpIDA is attractive since it can operate on a single image (it does not need a time-series) and hence can be applied to fixed samples. It can theoretically resolve the number of each oligomeric state present in an image, however this it at the loss of pixel-by-pixel resolution. The PCH approach can resolve multiple oligomeric states at a single point, however it is currently computationally too intensive to apply this method to each pixel of a large image series. The N&B approach is the only current approach capable of giving pixel-resolution oligomeric state information, but it is unable to delimit multiple co-located entities of different brightness: if a pixel contains entities of many brightnesses, the calculated brightness for that pixel will be some average of those brightnesses. This is related to an observation by Gambin et al. [32] that N&B cannot measure the size of rare large aggregates, but can report on their presence.

13. LSM-confocal microscopes for number and brightness

In their original paper, Digman and co-workers (Digman, 2008) utilized a LSM system equipped with a two photon excitation (2PE) Ti:Sapphire pulsed laser (Tsunami; Spectra Physics) and photon counting detectors. Commercial set ups have been used ever since; equipped with both photon counting detectors and analog detection.

14. Camera-based approaches for number and brightness

Number and Brightness has been carried out using Electron Multiplier Charged Couple Device (EM-CCD) cameras in combination with TIRF [4,5,33]. EM-CCD cameras have single-molecule sensitivity and a parallel mode of acquisition. They suffer from charge-well saturation and leakage and hence these devices require thorough characterization for correct N&B measurements. Two important effects of the issues with EM-CCDs are drift and nonlinearity [4]. The first can be solved by subtraction methods, the second limits the dynamic range of the brightness calculation and necessitates careful calculation of the S factor. Unruh and Gratton [4] give a detailed explanation of how to perform N&B analysis with EM-CCDs.

Scientific complementary metal-oxide semiconductor (sCMOS) cameras have advantages over EM-CCDs in speed, sensitivity and field of view. However, each pixel in an sCMOS camera has its own noise statistics. This makes N&B analysis with these devices extremely challenging and to date there are no publications applying N&B with sCMOS cameras. Recently, Liu et al. (2017) have developed an algorithm to correct images acquired with sCMOS cameras for this pixel-dependent noise. The result of this algorithm is a corrected image in units of photon counts. This could pave the way for the use of sCMOS camera images for N&B and many other FCS and FFS approaches.

It should be noted that camera-based acquisitions are subject to the same frame time and dwell time constraints as outlined above. With cameras, due to their parallel acquisition, the time spent acquiring a pixel is approximately equal to the time taken to acquire a whole frame. That makes the $t_{\text{frame}} \gg \tau_D \gg t_{\text{dwell}}$ requirement impossible to satisfy, so the frame time must be artificially increased by pausing between frames (or discarding frames) to increase t_{frame}.

Please cite this article in press as: R. Nolan et al., Methods (2017), https://doi.org/10.1016/j.ymeth.2017.12.001

15. Software and analysis

Graphical user interfaces (GUIs) for N&B analysis include *ZEN Black* (Zeiss), *SimFCS* (Laboratory for Fluorescence Dynamics, UC Irvine), and *Imaging FCS* [34]. Zeiss' software is limited in that it can only accept Zeiss' proprietary format as input for N&B analysis. SimFCS is an inexpensive commercial software offering many types of image analysis, however it is not well-documented and lacks functionality for outputting brightness image files (meaning that any post-brightness calculation analysis of the image must also be done inside SimFCS). Imaging FCS is a free ImageJ plugin which also provides many other image analysis algorithms. *nandb* [7] is an R package dedicated to number and brightness analysis. It is – so far – the only software to include the detrending algorithm which automatically selects the best detrend parameter [7]. As a textual interface, it is less intuitive but more mutable and extensible.

It should be noted that many extensions to the N&B technique are published merely with "in-house scripts" showing how the analysis was done. Without well-documented software packages, it is very difficult for others to adopt these techniques and as such, these in-house scripts are not enough. The people best-placed to create these packages are the inventors of these new methods (as they understand the new method best) and hence, for the good of the community, publications of these new methods should be accompanied by well-documented software packages such as python modules, R packages [35] or ImageJ plugins [36].

16. Concluding remarks

We have discussed the importance of quantifying protein interactions in live cells and given insights on the strengths and weaknesses of N&B. It is a very promising technique for the near future as it is able to perform very well with low photon budgets and therefore low expression levels in live cells. This is a feature shared with FCS and derivatives, but importantly, N&B is image-based and retrieves pixel-by-pixel information. Thanks to the implementation of gene-editing techniques, endogenous levels of labelled proteins are now available in many cell lines and this poses a big challenge for light microscopy from two perspectives: technological and analytical. The idea of using a straightforward approach in commercial set-ups already available in most biologically and medically oriented labs is very attractive. We stressed the importance of the residence time τ_D of the molecules under investigation: it should lie between the dwell time and the frame rate. Also, one clear limitation of the technique is that immobile entities limit the quantification possibilities. From the analytical point of view, the main challenge of the technique is to being able to correctly correct for bleaching. Our automatic detrending algorithm makes bleaching correction better and easier.

Acknowledgments

This work has been supported by Wellcome Trust grant 105278/Z/14/2 to R.N. The Wellcome Trust Centre for Human Genetics is funded by Wellcome Trust CORE Award 203852/Z/16/2.

Appendix A. Supplementary data

Supplementary data associated with this article can be found, in the online version, at https://doi.org/10.1016/j.ymeth.2017.12.001.

References

[1] M.A. Digman et al., Mapping the number of molecules and brightness in the laser scanning microscope, Biophys. J. 94 (6) (2008) 2320–2332.
[2] Q. Li et al., Single-particle tracking of human immunodeficiency virus type 1 productive entry into human primary macrophages, Acs Nano. 11 (4) (2017) 3890–3903.
[3] A.G. Palmer, N.L. Thompson, High-order fluorescence fluctuation analysis of model protein clusters, Proc. Natl. Acad. Sci. U.S.A. 86 (16) (1989) 6148–6152.
[4] J.R. Unruh, E. Gratton, Analysis of molecular concentration and brightness from fluorescence fluctuation data with an electron multiplied CCD camera, Biophys. J. 95 (11) (2008) 5385–5398.
[5] D.M. Jones et al., Dynamin-2 stabilizes the HIV-1 fusion pore with a low oligomeric state, Cell Rep. 18 (2) (2017) 443–453.
[6] K. Bacia, P. Schwille, Practical guidelines for dual-color fluorescence cross-correlation spectroscopy, Nat. Protoc. 2 (11) (2007) 2842–2856.
[7] R. Nolan et al., nandb—number and brightness in R with a novel automatic detrending algorithm, Bioinformatics (2017).
[8] S. Holmseth et al., Specificity controls for immunocytochemistry: the antigen preadsorption test can lead to inaccurate assessment of antibody specificity, J. Histochem. Cytochem. 60 (3) (2012) 174–187.
[9] H. Moriya, Quantitative nature of overexpression experiments, Mol. Biol. Cell. 26 (22) (2015) 3932–3939.
[10] D.A. Fortin et al., Live imaging of endogenous PSD-95 using ENABLED: a conditional strategy to fluorescently label endogenous proteins, J. Neurosci. 34 (50) (2014) 16698–16712.
[11] G.G. Gross et al., Recombinant probes for visualizing endogenous synaptic proteins in living neurons, Neuron 78 (6) (2013) 971–985.
[12] F.J. Mojica et al., Intervening sequences of regularly spaced prokaryotic repeats derive from foreign genetic elements, J. Mol. Evol. 60 (2) (2005) 174–182.
[13] L. Cong et al., Multiplex genome engineering using CRISPR/Cas systems, Science 339 (6121) (2013) 819–823.
[14] J.A. Doudna, E. Charpentier, Genome editing. The new frontier of genome engineering with CRISPR-Cas9, Science 346 (6213) (2014) 1258096.
[15] T. Mikuni et al., High-throughput, high-resolution mapping of protein localization in mammalian brain by in vivo genome editing, Cell 165 (7) (2016) 1803–1817.
[16] A.O. Khan et al., CRISPR-Cas9 mediated labelling allows for single molecule imaging and resolution, Sci. Rep. 7 (2017).
[17] S. Feng et al., Improved split fluorescent proteins for endogenous protein labeling, Nat. Commun. 8 (1) (2017) 370.
[18] X. Shi et al., Super-resolution microscopy reveals that disruption of ciliary transition-zone architecture causes Joubert syndrome, Nat. Cell Biol. (2017).
[19] H. Qian, E.L. Elson, Distribution of molecular aggregation by analysis of fluctuation moments, Proc. Natl. Acad. Sci. U.S.A. 87 (14) (1990) 5479–5483.
[20] R.B. Dalal et al., Determination of particle number and brightness using a laser scanning confocal microscope operating in the analog mode, Microsc. Res. Tech. 71 (1) (2008) 69–81.
[21] J.W. Krieger et al., Imaging fluorescence (cross-) correlation spectroscopy in live cells and organisms, Nat. Protoc. 10 (12) (2015) 1948–1974.
[22] K.H. Hur et al., Quantitative measurement of brightness from living cells in the presence of photodepletion, PLoS One 9 (5) (2014).
[23] K.H. Chan, J.C. Hayya, J.K. Ord, A note on trend removal methods: the case of polynomial regression versus variate differencing, Econometrica 45 (3) (1977) 737–744.
[24] P.J. Macdonald et al., Brightness analysis by Z-scan fluorescence fluctuation spectroscopy for the study of protein interactions within living cells, Biophys. J. 99 (3) (2010) 979–988.
[25] K.H. Hur, J.D. Mueller, Quantitative brightness analysis of fluorescence intensity fluctuations in E. Coli, PLoS One 10 (6) (2015).
[26] J. Hendrix et al., Pulsed interleaved excitation fluctuation imaging, Biophys. J. 105 (4) (2013) 848–861.
[27] M.A. Digman et al., Stoichiometry of molecular complexes at adhesions in living cells, Proc. Natl. Acad. Sci. U.S.A. 106 (7) (2009) 2170–2175.
[28] S. Padilla-Parra et al., Dual-color fluorescence lifetime correlation spectroscopy to quantify protein-protein interactions in live cell, Microsc. Res. Tech. 74 (8) (2011) 788–793.
[29] J. Hendrix, D.C. Lamb, Implementation and application of pulsed interleaved excitation for dual-color FCS and RICS, Methods Mol. Biol. 1076 (2014) 653–682.
[30] E. Hinde et al., Quantifying the dynamics of the oligomeric transcription factor STAT3 by pair correlation of molecular brightness, Nat. Commun. 7 (2016).
[31] M.A. Digman, E. Gratton, Imaging barriers to diffusion by pair correlation functions, Biophys. J. 97 (2) (2009) 665–673.
[32] Y. Gambin et al., Confocal spectroscopy to study dimerization, oligomerization and aggregation of proteins: a practical guide, Int. J. Mol. Sci. 17 (5) (2016).
[33] J.A. Ross et al., Oligomerization state of Dynamin 2 in cell membranes using TIRF and number and brightness analysis, Biophys. J. 100 (3) (2011) L15–L17.
[34] A.P. Singh, T. Wohland, Applications of imaging fluorescence correlation spectroscopy, Curr. Opin. Chem. Biol. 20 (Supplement C) (2014) 29–35.
[35] R. Core, R: A Language and Environment for Statistical Computing, 2017.
[36] J. Schindelin et al., The ImageJ ecosystem: an open platform for biomedical image analysis, Mol. Reprod. Dev. 82 (7–8) (2015) 518–529.